

# A Simplified Daylight Prediction Method for Designing Sawtooth Aperture

Kang-Soo Kim

Professor, Department of Architectural Eng., Korea University, Seoul, Korea

Jin-Mo Lee

Researcher, LG Engineering & Construction Technology Institute, Seoul, Korea

## Abstract

The sawtooth skylight is an excellent daylighting concept for the uniform interior illuminance over large working areas. In computer simulation, it is difficult for an architect to get accurate daylight illuminances for the spaces where sawtooth apertures are applied. In this study, daylight prediction algorithms for sawtooth apertures are developed. The flux transfer method is applied for this study to predict daylight illuminances. The simplified equations from this study can be used effectively for preliminary prediction of daylight in sawtooth spaces.

**Keywords:** daylight, flux transfer method, sawtooth aperture, luminance ratio, SUPERLITE

## 1. INTRODUCTION

Toplighting concepts through apertures have been used in deep interior areas to support the sidelighting concepts. Sawtooth apertures which have been normally applied to the roofs of industrial and commercial spaces are nowadays more used to the roof of general spaces. The sawtooth apertures are excellent daylighting concepts for the uniform interior illuminance over large working areas. Traditionally, a scale model testing method has been used to predict the daylight illuminance for particular tolighted spaces. In computer simulation, it is difficult for an architect to get accurate daylight illuminances for the spaces where sawtooth apertures are applied. In this study, daylight prediction algorithms for sawtooth apertures are developed. This simplified equations can be used effectively for an architect to predict daylight illuminances under uniform and overcast skies in the early design phase.

## 2. THE FLUX TRANSFER METHOD

The flux transfer method can be used to decide the flux transfer as a configuration factor from a luminance source surface to a small target plane or the flux transfer as a form factor from a luminance source to a second luminance surface. The configuration factor  $C$  is the ratio of the illuminance at a small target plane to the luminous existence of a luminance surface. For parallel surfaces, the configuration factor  $C_H$  is defined as following equation.

$$C_H = \frac{1}{2\pi} \left( \frac{x}{\sqrt{z^2 + x^2}} \tan^{-1} \frac{y}{\sqrt{z^2 + x^2}} + \frac{y}{\sqrt{z^2 + y^2}} \tan^{-1} \frac{x}{\sqrt{z^2 + y^2}} \right) \quad \text{--(Eq.1)}$$

If the target plane is normal to the source surface, the configuration factor  $C_V$  is defined as follows.

$$C_V = \frac{1}{2\pi} \left( \tan^{-1} \frac{x}{z} - \frac{z}{\sqrt{z^2 + y^2}} \tan^{-1} \frac{x}{\sqrt{z^2 + y^2}} \right) \quad \text{--(Eq.2)}$$

In the above equation,  $x$  and  $y$  describe the source surface, and  $z$  describes the distance from the surface to the target plane.

## 3. CALCULATION METHOD FOR SAWTOOTH APERTURES

In this study, the flux transfer method is applied to predict daylight illuminances. In the flux transfer method, the target plane is either normal or parallel to the source surface. In order to use the configuration factor  $C$ , accurate source area is calculated first. In this daylight prediction study, the daylight component through the apertures can be divided into sky components (SC), and reflected components such as the internal reflectance component (IRC) and the external reflectance component (ERC). From the viewpoint of target plane, aperture windows are vertical sources and the projected areas of inside reflectors are parallel sources (Figure 1, Figure 2). Internal reflectance components between walls which are located under apertures are not included in this study.

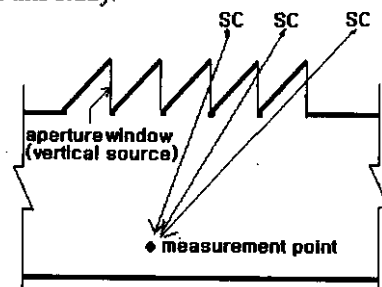


Figure 1. Sky components

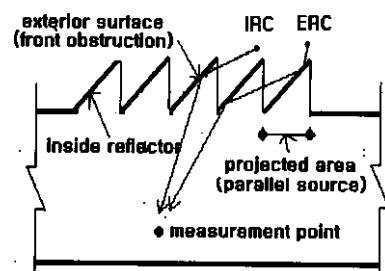


Figure 2. Reflected components

3.1 Calculation of Sky Component

The sky component is calculated by the configuration factor C for the normal surface to the target plane. Therefore, visible window areas need to be calculated first. The window area which can be seen from the measurement point is calculated by multiplying the window width by the visible window height. Visible window height is much related with the obstruction effect of the front aperture. If another aperture is located in front of one skylight, much obstruction effect exists to the original window height. For the sky component calculation through computer, the visible sky area needs to be divided into the small square areas. Then, the luminance of each sky segment is calculated and summed to get the total sky luminances that are visible from the measurement points. In this study, sky component equations are developed for the uniform and the overcast sky conditions. In the overcast sky conditions, luminance variances between the zenith and the horizon are carefully considered.

3. 1. 1 Aperture without front obstruction

In the case of aperture without front obstructions (Figure 3), the height of aperture can be calculated with geometric correlations between the aperture and the measurement point. The term  $P_{ST}$ , and  $A_{ST}$  represent reference point and reference distance. And the term P and A mean measurement point and distance of measurement point. RH means room height. WH, HL and HS are shown in Figure 3. WH is the floor-to-work surface height. HL is the work surface-to-ceiling height (to the bottom of the aperture). The term  $\theta$  represents angle of slopped roof of sawtooth aperture.  $A_{ST}$  can be calculated by Eq. 3. Locations of the measurement points (P) regarding to  $A_{ST}$  can be calculated with the data of HH; height of visible window seen from the measurement point (table 1., Figure 4). In this calculation, each segment of sky luminance needs to be accumulated for getting a total sky luminance seen from the visible window.

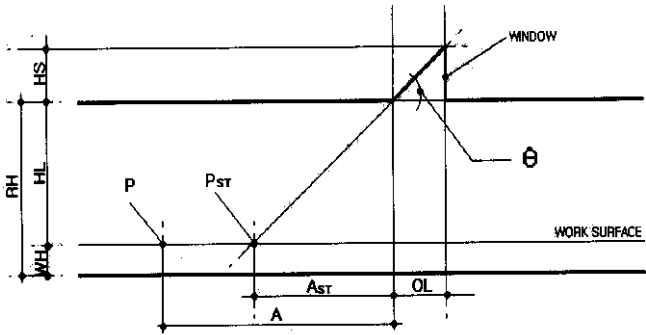


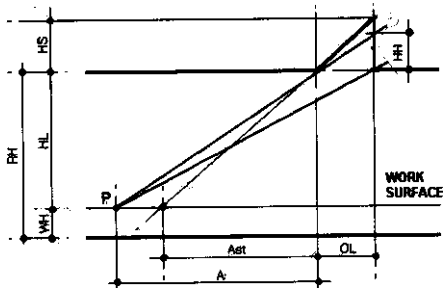
Figure 3. Reference points and distances (without front obstruction)

$A_{ST} : HL = OL : HS$   
 $OL = \frac{HS}{\tan \theta} \therefore A_{ST} = \frac{HL}{\tan \theta}$  -----(Eq. 3)

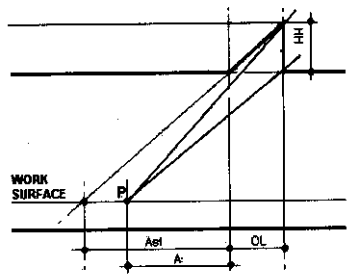
Table 1. Equations for HH without front obstruction

| A                     | HH  |               |
|-----------------------|---|---------------|
| $A = A_{ST}$          | $HH = HS$   | Figure 3.     |
| $A > A_{ST}$          | $HH = \frac{HL}{A} \times \frac{HS}{\tan \theta}$ | Figure 4-(a). |
| $A_{ST} \geq A > -OL$ | $HH = HS$   | Figure 4-(b). |
| $-OL \geq A$          | $HH = 0$  | Figure 4-(c). |

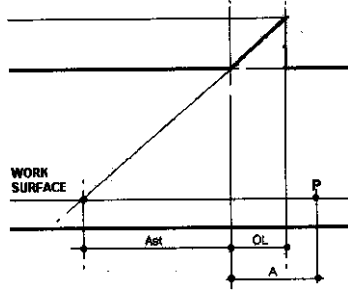
A : Distance of measurement point  
HH : Height of window seen from the measurement point



(a) Partly visible sky



(b) Full sky



(c) Invisible sky

Figure 4. Sawtooth aperture visible from the measurement point without front obstruction

3. 1. 2 Aperture with front obstruction

If more than one aperture is installed on the roof, the first aperture in a series will not have front obstruction. However, if the second aperture has front obstruction (exterior surface of slopped roof.), the height of visible window seen from the measurement point will be decreased. Reference distances( $A_{st2}$ ,  $A_{st3}$ ) are shown in Figure 5. Calculation equations for  $A_{st2}$  and  $A_{st3}$  are shown in Eq.4 and Eq.5. Equations for the height of visible window seen from the measurement point(HH) are shown in Table 2. Sawtooth aperture classifications with front obstructions are shown in Figure 6.

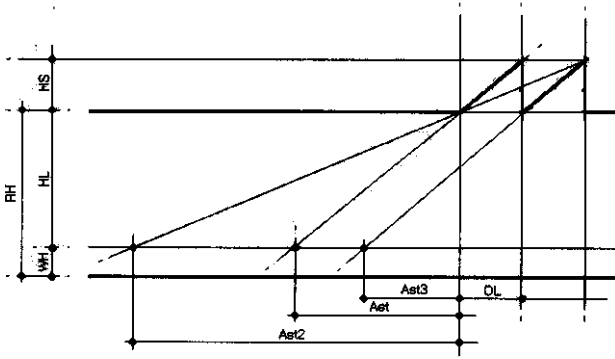


Figure 5. Reference points and distances (with front obstruction)

$$\frac{A_{ST}^2}{HL} = \frac{2 \times OL}{HS} \quad \therefore A_{ST}^2 = \frac{2 \times HS}{\tan \theta} \times HL \times \frac{1}{HS} = \frac{2 \times HL}{\tan \theta} \quad \text{---(Eq. 4)}$$

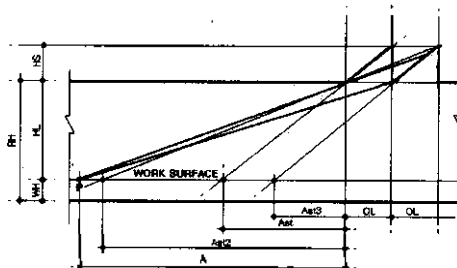
$$A_{ST}^3 = A_{ST} - OL \quad \text{---(Eq. 5)}$$

where  $\theta$ : Angle of sloped roof of sawtooth aperture (Figure 3).

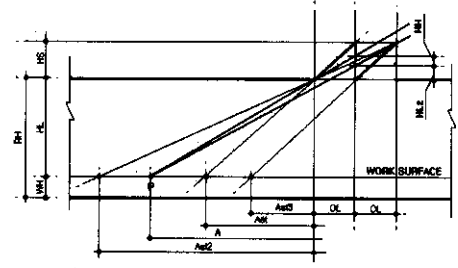
Table 2. Equations for HH with front obstruction

| A                            | HH  |               |
|------------------------------|---|---------------|
| $A = A_{ST}^2$               | $HH = 0$  | Figure 5.     |
| $A = A_{ST}^3$               | $HH = HS$   |               |
| $A \geq A_{ST}^2$            | $HH = 0$  |               |
| $A_{ST}^2 > A > A_{ST}^3$    | $\frac{HL_2 + HL}{HS} = \frac{HL + HS}{A + \frac{2 \times HS}{\tan \theta}}$  | Figure 6-(b). |
|                              | $HL_2 = \frac{A \times \tan \theta + HS}{A \times \tan \theta + 2 \times HS} \times (HL + HS) - HL$   |               |
|                              | $HH + HL_2 = \frac{HL}{A} \times \frac{HS}{\tan \theta}$  |               |
| $A_{ST}^3 \geq A > A_{ST}^3$ | $\therefore HH = \frac{HL}{A} \times \frac{HS}{\tan \theta} - \frac{A \times \tan \theta + HS}{A \times \tan \theta + 2 \times HS} \times (HL + HS) + HL$ | Figure 6-(c). |
|                              | $\frac{HL_2 + HL}{HS} = \frac{HL + HS}{A + \frac{2 \times HS}{\tan \theta}}$  |               |
|                              | $HL_2 = \frac{A \times \tan \theta + HS}{A \times \tan \theta + 2 \times HS} \times (HL + HS) - HL$   |               |
| $A_{ST}^3 \geq A > -OL$      | $HH + HL_2 = HS$  | Figure 6-(d). |
|                              | $\therefore HH = HS - HL_2 = (HL + HS) \times \frac{HS}{A \times \tan \theta + 2 \times HS}$  |               |
|                              | $HH = HS$   |               |
| $-OL \geq A$                 | $HH = 0$  |               |

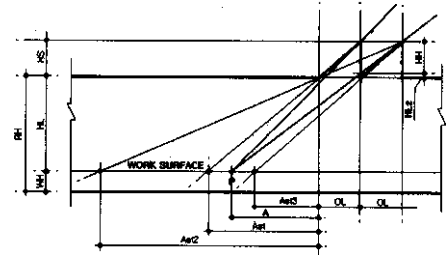
Where  $HL_2$ : Height of windows shaded by the front aperture (Figure 6).



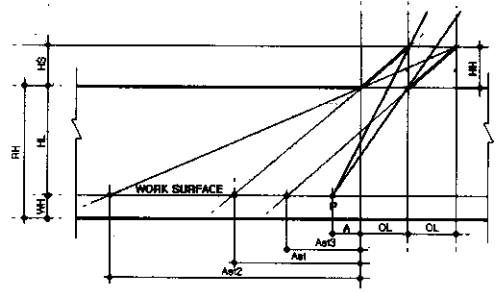
(a) Invisible sky



(b) Partly visible sky



(c) Partly visible sky



(d) Full sky

Figure 6. Sawtooth aperture visible from the measurement point with front obstruction

### 3.2 Calculation of Reflected Components

The daylight components that affect inside reflectors of sawtooth aperture are sky components from the sky (IRC) and reflected components from the exterior surface of front aperture (ERC). Inside reflector means the interior surface of sloped roof of sawtooth aperture. In this part, reflected components are calculated with 1500 SUPERLITE IEA 2.0 simulations. Luminance ratios for inside reflectors are calculated for the case of aperture with and without obstruction under uniform and overcast sky conditions (Table 3). Sloped angle variables of  $45^\circ$ ,  $30^\circ$  and  $15^\circ$  are selected for simulations. The sawtooth aperture types are classified into 6 cases regarding the ratios between window height (HS) and window length (L). The average luminances of inside reflectors can be calculated by converting luminance ratios to luminances. The term  $L_1$  and  $L_2$  represent average luminance of inside reflector and zenith luminance (Eq. 6). The average of  $L_1$  is calculated by SUPERLITE simulation and  $L_2$  is calculated by Eq. 7.

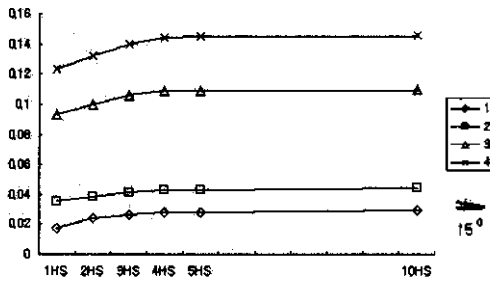
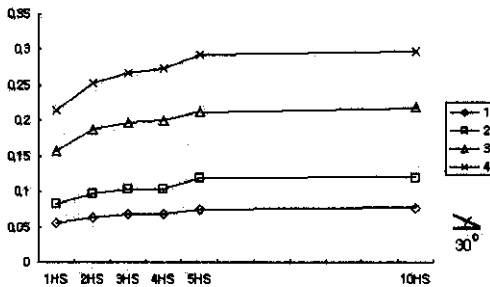
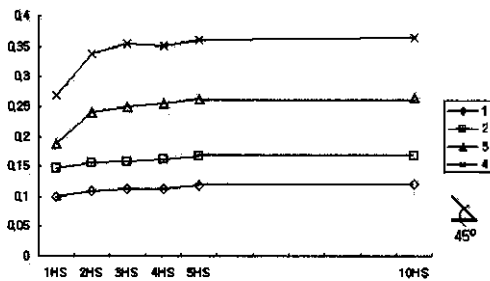
$$\text{Luminance Ratio for inside reflector} = L_1 / L_2 \quad (\text{lm/lm}) \quad \text{---(Eq. 6)}$$

$$L_2 = 0.123 + 8.6 \sin(\phi) \quad (\text{lm}) \quad \text{---(Eq. 7)}$$

Where  $\phi$ : the altitude of sun

Table 3. Luminance Ratios for inside reflector

| $\theta$ | L    | Without front obstruction |                   | With front obstruction |                   |
|----------|------|---------------------------|-------------------|------------------------|-------------------|
|          |      | Under Overcast sky        | Under Uniform sky | Under Overcast sky     | Under Uniform sky |
| 45°      | 1HS  | 0.099                     | 0.146             | 0.187                  | 0.268             |
|          | 2HS  | 0.109                     | 0.155             | 0.241                  | 0.338             |
|          | 3HS  | 0.112                     | 0.157             | 0.250                  | 0.354             |
|          | 4HS  | 0.113                     | 0.161             | 0.256                  | 0.351             |
|          | 5HS  | 0.119                     | 0.167             | 0.262                  | 0.361             |
|          | 10HS | 0.120                     | 0.168             | 0.265                  | 0.365             |
| 30°      | 1HS  | 0.055                     | 0.083             | 0.158                  | 0.215             |
|          | 2HS  | 0.063                     | 0.097             | 0.187                  | 0.253             |
|          | 3HS  | 0.068                     | 0.103             | 0.197                  | 0.268             |
|          | 4HS  | 0.069                     | 0.103             | 0.201                  | 0.274             |
|          | 5HS  | 0.075                     | 0.119             | 0.213                  | 0.292             |
|          | 10HS | 0.077                     | 0.120             | 0.220                  | 0.298             |
| 15°      | 1HS  | 0.017                     | 0.035             | 0.093                  | 0.123             |
|          | 2HS  | 0.024                     | 0.038             | 0.100                  | 0.132             |
|          | 3HS  | 0.026                     | 0.041             | 0.106                  | 0.140             |
|          | 4HS  | 0.028                     | 0.043             | 0.109                  | 0.144             |
|          | 5HS  | 0.028                     | 0.043             | 0.109                  | 0.145             |
|          | 10HS | 0.029                     | 0.044             | 0.110                  | 0.146             |

(a)  $\theta = 15^\circ$ (b)  $\theta = 30^\circ$ (c)  $\theta = 45^\circ$ 

Case 1  $\blacklozenge$ : Without front obstruction under Overcast sky  
 Case 2  $\blacksquare$ : Without front obstruction under Uniform sky  
 Case 3  $\blacktriangle$ : With front obstruction under Overcast sky  
 Case 4  $\blackcross$ : With front obstruction under Uniform sky

Figure 7. Tendencies of luminance Ratios for inside reflector

Figure 7 shows the tendencies of luminance ratios in different sloped angles which can be used in early design steps. In each graph, x-axis shows widths of sawtooth (L, Figure 8) and y-axis shows luminance ratios. Luminance ratios under the uniform sky (case 2, 4) are higher than those under the CIE overcast sky (case 1, 3). The reason is that the luminances of visible sky from the inside reflector under the uniform sky are higher than those under the CIE overcast sky.

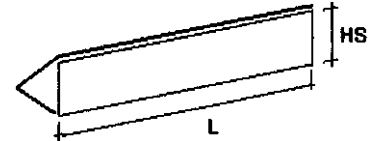


Figure 8. Width (L) and height (HS) of sawtooth

Another tendency is that the luminance ratios with front obstruction (case 3, 4) are higher than those without obstruction (case 1, 2). In case of aperture with front obstruction, the inside reflector has another reflector (exterior surface of front sawtooth), (Figure 2).

The luminance of inside reflector is calculate by Eq 8, 9

In case of aperture without front obstruction :

Luminance of inside reflector =  $L_z \times \text{Luminance Ratios} \times \text{Reflectance of inside reflector (\%)} \dots \dots \dots \text{(Eq. 8)}$

In case of aperture with front obstruction :

Luminance of inside reflector =  $L_z \times \text{Luminance Ratios} \times \text{Reflectance of inside reflector (\%)} \times \text{Reflectance of exterior surface of reflector (\%)} \dots \dots \dots \text{(Eq. 9)}$

The calculated luminances can be divided into the following 4 cases as shown in Table 4 and Figure 9. As the inside reflector is not seeing from the measurement point in 9-(a), projected areas ( $OL \times RW$  (room width)) of inside reflectors are regarded as overhead light sources. Then, the configuration factors of C for parallel surfaces are applied for these projected areas. Luminances of insider reflectors are calculated by multiplying luminance ratios in Table 3 with zenith luminances (Eq.8, Eq.9). Same process can be applied in different cases shown in Figure 9.

Table 4. Calculations of configuration factors according to the relation between measurement point and inside reflector

| A   | $\Sigma C_i$ (Configuration Factors)           |               |
|---|--|---------------|
| $A > A_{ST}$                                | 0  | Figure 9-(a). |
| $A_{ST} \geq A \geq 0$                      | $C_H(OL_1 + OL_2, RW, HL)$ $C_H(OL_3, RW, HL)$ | Figure 9-(b). |
| $0 \geq A > -OL (= \frac{HS}{\tan \theta})$ | $C_H(OL_1, RW, HL) + C_H(OL_2, RW, HL)$        | Figure 9-(c). |
| $-OL \geq A$                                | $C_H(OL_2 + OL_4, RW, HL) - C_H(OL_4, RW, HL)$ | Figure 9-(d). |

where  $C_H$  : Configuration factor for parallel surface (Eq.1)  
 $\Sigma C$  : Summation of configuration factors  
 RW : Room Width

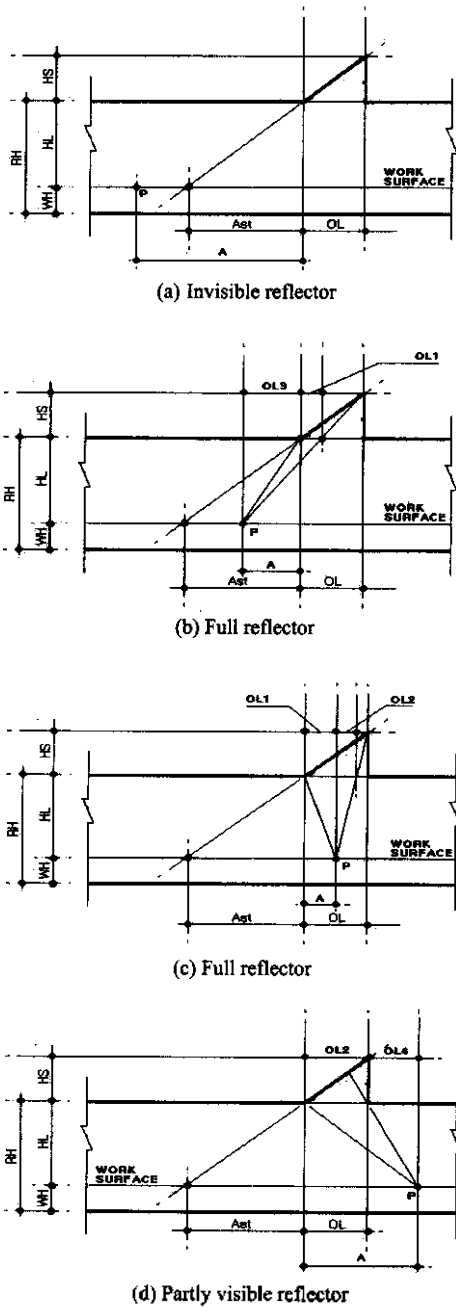


Figure 9. Inside reflector visible from the measurement point

The illuminance at the measurement point ( $E_p$ ) is calculated by following equations (Eq10, 11, 12)

$$E_{direct} = L_z \times \sum C_v \times \text{Transmittance of aperture window} \quad \text{-----(Eq.10)}$$

$$E_{reflected} = \sum (L_R \times \sum C_r) \times \text{Transmittance of aperture window} \quad \text{-----(Eq.11)}$$

$$E_p = E_{direct} + E_{reflected} \quad \text{-----(Eq.12)}$$

where

$\sum C_v$  : The sum of configuration factors of visual vertical sources (Eq.2)

$L_R$  : The luminance of inside reflector (Eq.8, 9)

$\sum C_r$  : The sum of configuration factors of visual parallel sources (Eq.1, Table 4)

### 3.3 Comparison results

The calculation method developed in this study is programmed through visual basic language (Figure10).

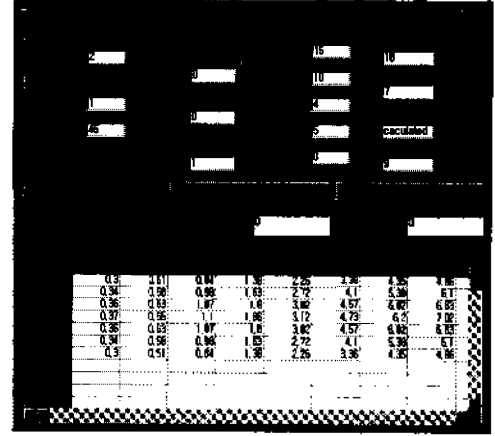


Figure 10. Input & Output interface of developed program

Developed algorithms in this study are limited to the case that room width (RW) is equal to window length (L), (Figure 11). Then, the data from this study are compared with SUPERLITE data and the scale model data. Dimensions of the original space are as follows: 1) room length (RL); 15m, 2) room width (RW); 10m, 3) room height (RH); 5m. For the comparison, scale model was constructed with the scale of 1:20. Scale model data were obtained on the roof of Engineering building at K University in Seoul and exterior illuminance was 10,000~12,000 Lux. Figure 11-(a) and 11-(b) show the model spaces with and without front obstruction. 18 measurement points were selected at the centerline on work surface, and the height of work-surface (WH) was 1m and the reflectance of inside reflector was 80%.

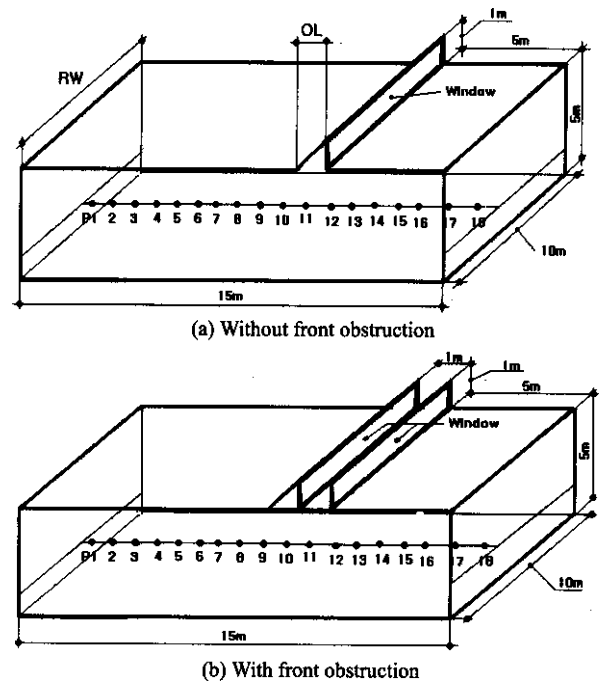


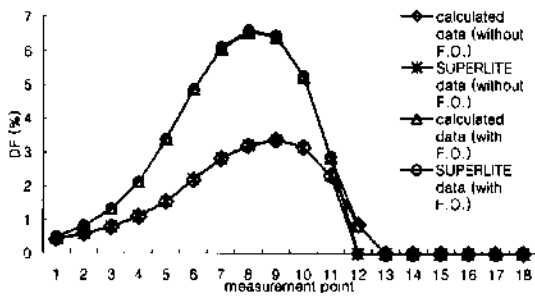
Figure 11. Scale models

### 3.3.1 Comparison of Sky Components

The sky components calculated from this study are compared with SUPERLITE data and the scale model data.

#### a) Uniform Sky

The calculated data from this study are compared with SUPERLITE data. In the case of aperture without obstruction, the absolute difference between the calculated data and SUPERLITE data is 0.06 DF. In the case of aperture with obstruction, the absolute difference between the calculated data and SUPERLITE data is 0.06 DF (Figure 12).



Where F.O. : front obstruction

Figure 12. Comparison of sky components (uniform sky)

#### b) CIE Overcast Sky

In the case of aperture without obstruction, the absolute difference between the calculated data and SUPERLITE data is 0.06 DF, and also, the absolute difference between the calculated data and scale model data is 0.10 DF. Also, In the case of aperture with obstruction, the absolute difference between the calculated data and SUPERLITE data is 0.7DF, and also, the absolute difference between the calculated data and scale model data is 0.2 DF (Figure 13).

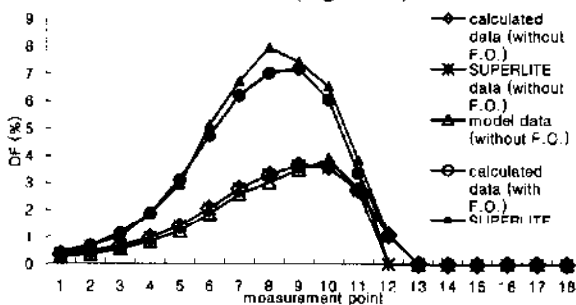


Figure 13. Comparison of sky components (overcast sky)

### 3.3.2 Comparison of Reflected Components (CIE overcast sky)

The reflected components data calculated from this study are compared with the scale model data. Sky condition is limited to the case of CIE overcast sky. In the case of aperture without obstruction, the absolute difference between the calculated data and the scale model data is 0.13 DF. In the case of skylight with obstruction, the absolute difference between the calculated data and scale model data is 0.14 DF (Figure 14).

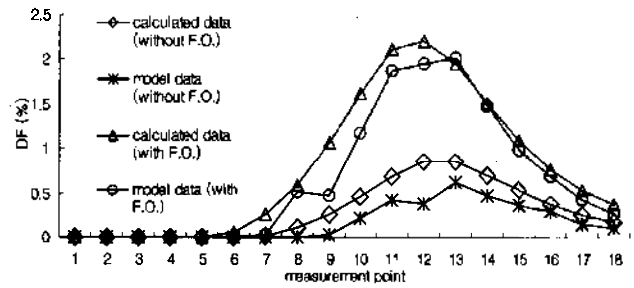


Figure 14. Comparison of reflected components (overcast sky)

### 3.3.3 Comparison of Total Components (Sky Components + Reflected Components, CIE overcast sky)

In the case of aperture without obstruction, the absolute difference between the calculated data and the scale model data is 0.2 DF. Also, In the case of skylight with obstruction, the absolute difference between the calculated data and the scale model data is 0.19 DF (Figure 15).

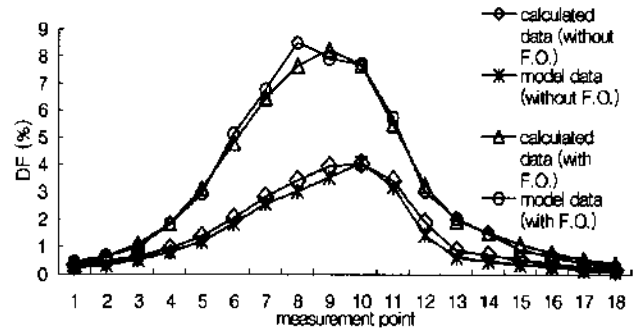


Figure 15. Comparison of total components (overcast sky)

## 4. CONCLUSION

A daylight prediction method for sawtooth apertures is presented in this study. For the sky component calculation, vertical window areas and sky luminances should be calculated first. Also, inside areas and luminances of apertures should be calculated to use the flux transfer method. Calculation algorithms developed in this study have been validated through the comparison with SUPERLITE data and the scale model data. The simplified program developed in this study can be used effectively for the preliminary prediction of daylight in sawtooth spaces.

## REFERENCES

- Frederic k C. et al. (1985) Daylighting Simulation in the DOE-2 Building Energy Analysis Program, Energy and buildings, Vol. 8, pp.271-286.
- Fuller Moore. (1985) Concept and practice of architectural daylighting, VNR Co.
- Gregg D. Ander. (1995) Daylighting Performance and Design, VNR Co.
- Kim K.S. et al. (1997) Daylighting Prediction and Measurement of Underground Spaces, ISES 1997 Solar World Congress: 392-399.
- Robbins, C. L. (1986) Daylighting, VNR Co., pp. 203-220.